



CTEQ

Review of Parton Distribution Function

Tie-Jiun Hou
In collaboration with CTEQ-TEA

Southern Methodist University

August 04, DPF2015 at UM,
Ann Arbor, MI

CTEQ-TEA group

- CTEQ – Tung et al. (TEA)
in memory of Prof. Wu-Ki Tung, who established CTEQ
Collaboration in early 90's.
- Current members:
Sayipjamal Dulat (Xinjiang U.)
Tie-Jiun Hou, Pavel Nadolsky (Southern Methodist U.)
Jun Gao(Argonne Nat. lab.)
Marco Guzzi(U. of Manchester)
Joey Huston, Jon Pumplin, Carl Schmidt,
Dan Stump, C.-P. Yuan(Michigan State U.)

Hadron Collider Physics

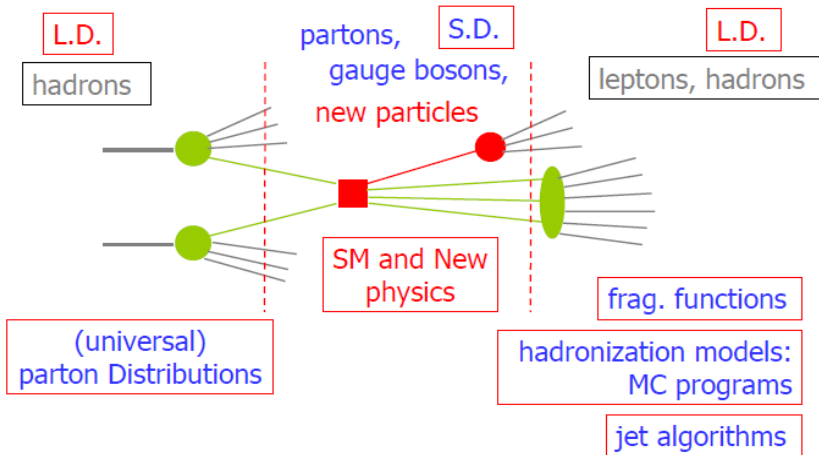


Table by A.Accardi,
DIS'2015 workshop

	JLab	HERA I+II <i>Wichmann</i>	Tevatron new W,Z	LHC	di- μ	Nucl.	HT TMC	Flex d	closure
NEW: HERAPDF2.0 → <i>Myronenko, Brandt</i>		✓	☒						
NEW: CT14 → <i>Nadolski</i>			✓ ☒☒	✓	✓			✓	
NEW: MMHT14 → <i>Thorne</i>			✓ ☒☒	✓	✓	✓			
NEW: NNPDF3.0 → <i>Deans</i>				✓	✓				✓
[GJR14]	✓			✓	✓	✓	✓		
CJ12 * (→ CJ15) → <i>Melnitchouk</i>	✓	(✓)	(✓)		✗	✓	✓	✓	
ABM12 **					✓	✓	✓		

* NLO only ** No jet data ☒ but see 1503.05221 ☒☒ no reconstructed W

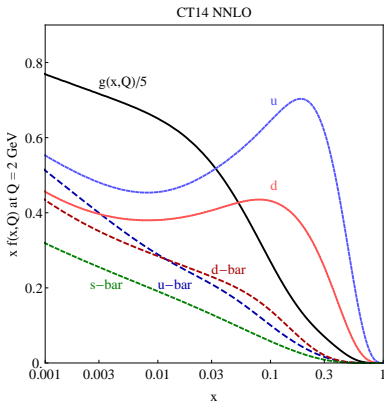
CT14 NNLO error PDFs

Available at <http://hep.pa.msu.edu/cteq/public/index.html>, is being submitted to LHAPDF;

- CT10 includes only pre-LHC data
- CT14 is the first CT analysis including LHC Run 1 data
- CT14 also includes the new Tevatron D0 Run 2 data on W-electron charge asymmetry
- CT14 uses a more flexible parametrization in the non-perturbative PDFs.

CT14 NNLO

2 GeV



100 GeV

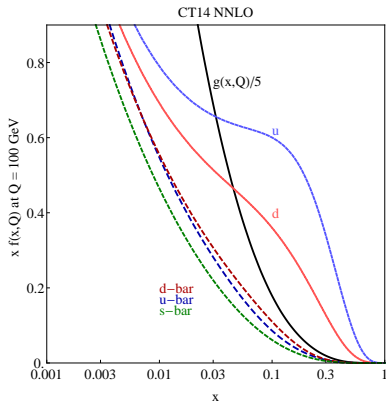


Figure 1: The CT14 parton distribution functions at $Q = 2 \text{ GeV}$ and $Q = 100 \text{ GeV}$ for $u, \bar{u}, d, \bar{d}, s = \bar{s}$, and g .

DGLAP evolution for PDFs

- Non-perturbative PDFs are determined at the scale of $Q=1.3$ GeV.
- PDFs at any other scale Q can be obtained from PQCD, via solving DGLAP evolution equations.
- Due to DGLAP evolution, the PDF error band becomes smaller when the energy scale Q increases.
- The evolution effect is large in low Q region, say, from 1.3 GeV to 8 GeV.

The CT14-NNLO global analysis of QCD

Parametrization of PDFs $Q = 1.3$ GeV, with 28 parameter values to be chosen; there are from 4 to 6 parameters for each proton type.

Many data sets, for short distance interactions.

Perturbative QCD, using NNLO approximations whenever available.

Taking account of **experimental errors**, statistical and systematic. (Not so strong on systematic **theoretical errors**).

ID#	Experimental data set	N_{pt}	χ_e^2	χ_e^2/N_{pt}	S_n
101	BCDMS F_2^P	337	384	1.14	1.74
102	BCDMS F_2^d	250	294	1.18	1.89
104	NMC F_2^d/F_2^P	123	133	1.08	0.68
106	NMC σ_{red}^P	201	372	1.85	6.89
108	CDHSW F_2^P	85	72	0.85	-0.99
109	CDHSW F_3^P	96	80	0.83	-1.18
110	CCFR F_2^P	69	70	1.02	0.15
111	CCFR $\times F_3^P$	86	31	0.36	-5.73
124	NuTeV $\nu\mu\mu$ SIDIS	38	24	0.62	-1.83
125	NuTeV $\bar{\nu}\mu\mu$ SIDIS	33	39	1.18	0.78
126	CCFR $\nu\mu\mu$ SIDIS	40	29	0.72	-1.32
127	CCFR $\bar{\nu}\mu\mu$ SIDIS	38	20	0.53	-2.46
145	H1 σ_r^b	10	6.8	0.68	-0.67
147	Combined HERA charm production	47	59	1.26	1.22
159	HERA1 Combined NC and CC DIS	579	591	1.02	0.37
169	H1 F_L	9	17	1.92	1.7

ID#	Experimental data set	N_{pt}	χ_e^2	χ_e^2/N_{pt}	S_n
201	E605 Drell-Yan process	119	116	0.98	-0.15
203	E866 Drell-Yan process, $\sigma_{pd}/(2\sigma_{pp})$	15	13	0.87	-0.25
204	E866 Drell-Yan process, $Q^3 d^2\sigma_{pp}/(dQdx_F)$	184	252	1.37	3.19
225	CDF Run-1 electron $A_{ch}, p_{T\ell} > 25$ GeV	11	8.9	0.81	-0.32
227	CDF Run-2 electron $A_{ch}, p_{T\ell} > 25$ GeV	11	14	1.24	0.67
234	DØ Run-2 muon $A_{ch}, p_{T\ell} > 20$ GeV	9	8.3	0.92	-0.02
240	LHCb 7 TeV $35 \text{ pb}^{-1} W/Z d\sigma/dy_\ell$	14	9.9	0.71	-0.73
241	LHCb 7 TeV $35 \text{ pb}^{-1} A_{ch}, p_{T\ell} > 20$ GeV	5	5.3	1.06	0.30
260	DØ Run-2 Z rapidity	28	17	0.59	-1.71
261	CDF Run-2 Z rapidity	29	48	1.64	2.13
266	CMS 7 TeV 4.7 fb^{-1} , muon $A_{ch}, p_{T\ell} > 35$ GeV	11	12.1	1.10	0.37
267	CMS 7 TeV 840 pb^{-1} , electron $A_{ch}, p_{T\ell} > 35$ GeV	11	10.1	0.92	-0.06
268	ATLAS 7 TeV $35 \text{ pb}^{-1} W/Z$ cross sec., A_{ch}	41	51	1.25	1.11
281	DØ Run-2 9.7 fb^{-1} electron $A_{ch}, p_{T\ell} > 25$ GeV	13	35	2.67	3.11
504	CDF Run-2 inclusive jet production	72	105	1.45	2.45
514	DØ Run-2 inclusive jet production	110	120	1.09	0.67
535	ATLAS 7 TeV 35 pb^{-1} incl. jet production	90	50	0.55	-3.59
538	CMS 7 TeV 5 fb^{-1} incl. jet production	133	177	1.33	2.51

34 data sets used for the CT14-NNLO global analysis.

Experimental uncertainty

An experiment publishes N measurements,

$$\{M_i; i = 1, 2, 3, \dots, N\}$$

Each measurement has several parts,

$$\begin{aligned} M_i &= \{D_i; \sigma_{0i}; \{\sigma_{1i}, \sigma_{2i}, \sigma_{3i}, \dots\}\} \\ &= \{\text{center value; SD of statistical error;} \\ &\quad \text{SDs of correlated systematic errors}\} \end{aligned}$$

that is,

$$D_i = \text{True}_i + \sigma_{0i} r_0 + \sum_{k=1}^{N_{\text{sy}}} \sigma_{ki} r_k$$

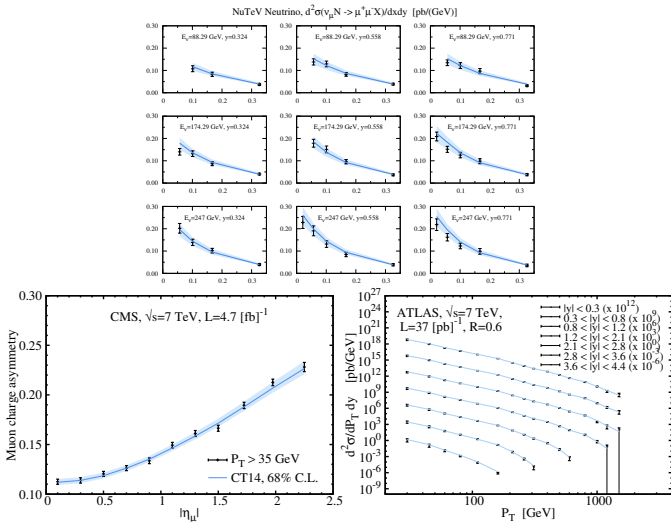
Where r_0 and $\{r_k\}$ are random variables (gaussian?).

Define

$$\chi_{\text{global}}^2 = \sum_i \frac{[D_i - \sum_k r_k \sigma_{ki} - T_i(a)]^2}{\sigma_{0i}^2} + \sum_k r_k^2.$$

and minimize with respect to both the normalized systematic shifts $\{r_k\}$ and the theory parameters.

CT14 NNLO v.s. fitted data

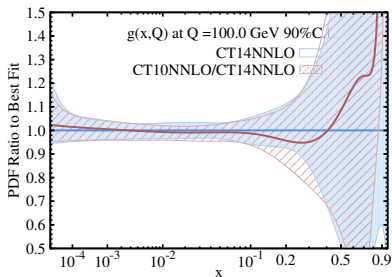
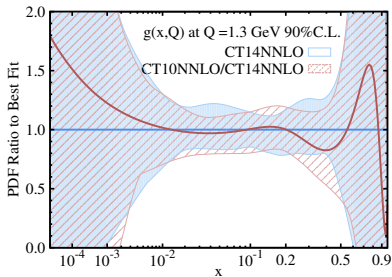
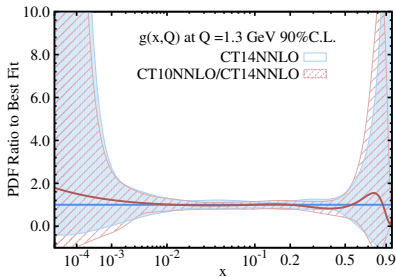


Fit well: $\chi^2/N_{pt} = 3252/2947 = 1.10$

CT14 NNLO PDFs

- PDF error bands
 - u and d PDFs are best known
 - currently, no strong constraint for x below $1E-4$
 - large error for x above 0.3
 - large sea (e.g. \bar{u} and \bar{d}) quark uncertainties in large x region
 - with non-perturbative parametrization form dependence in small and large x regions
- PDF eigensets
 - useful for calculating PDF induced uncertainty

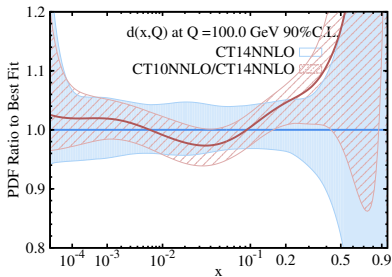
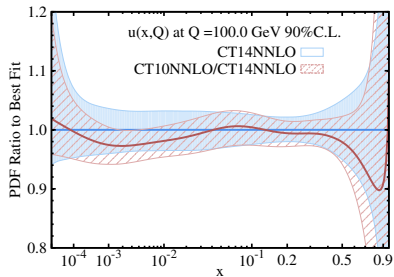
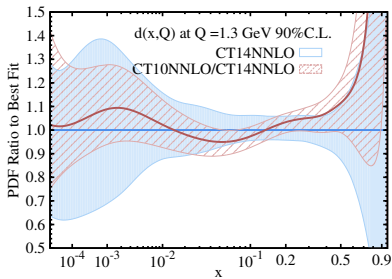
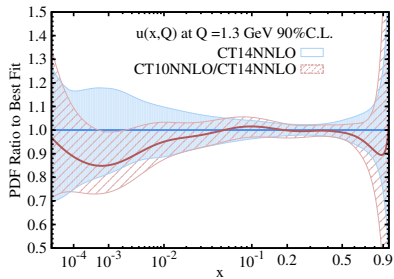
CT14 and CT10 NNLO PDFs



CT14 and CT10 NNLO PDFs

$u(x, Q)$

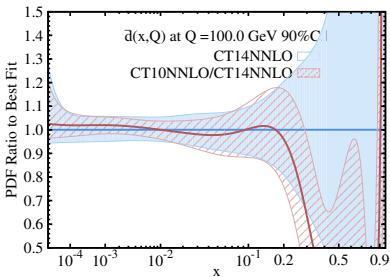
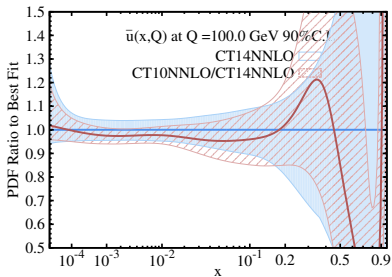
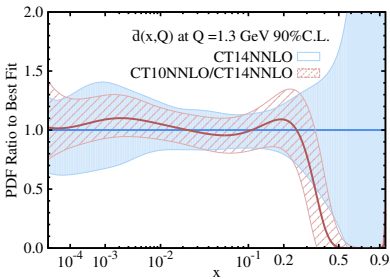
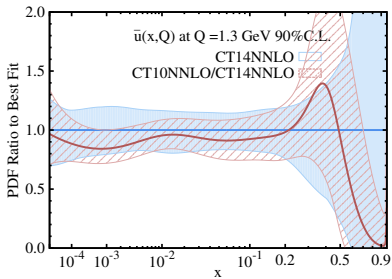
$d(x, Q)$



CT14 and CT10 NNLO PDFs

$$\bar{u}(x, Q)$$

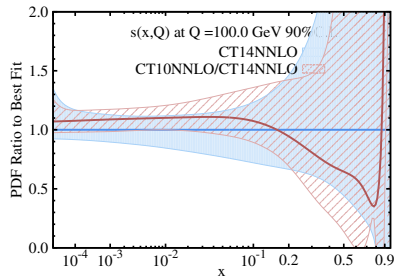
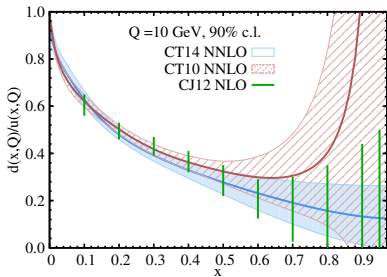
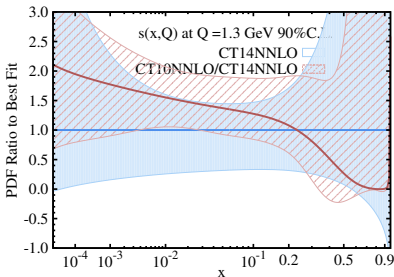
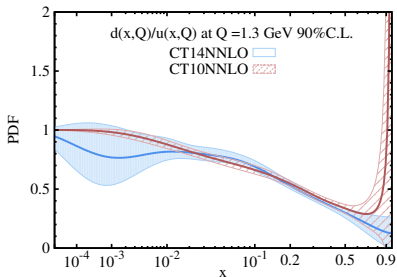
$$\bar{d}(x, Q)$$



CT14 and CT10 NNLO PDFs

$$d(x, Q)/u(x, Q)$$

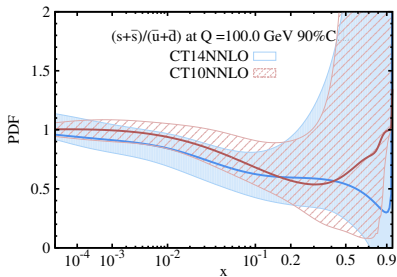
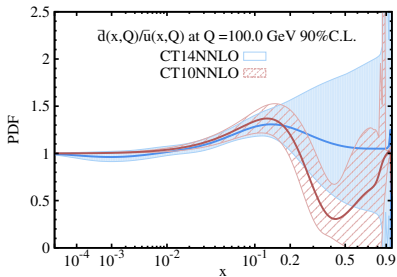
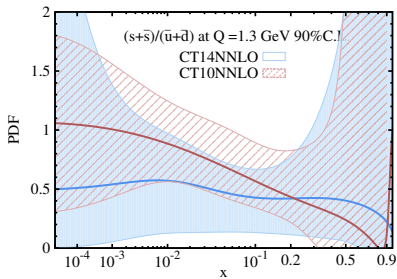
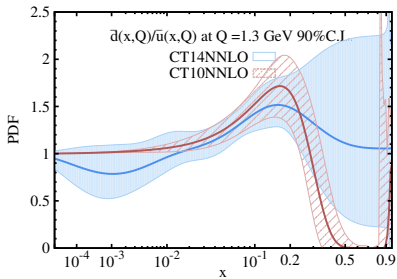
$$s(x, Q)$$



CT14 and CT10 NNLO PDFs

$$\bar{d}(x, Q)/\bar{u}(x, Q)$$

$$(s + \bar{s})/(\bar{u} + \bar{d})$$



NNLO cross section and PDF induced uncertainty for $gg \rightarrow H$

$$\Delta\sigma_{\text{PDF}} = \frac{1}{2} \sqrt{\sum_{i=1}^n \left(\sigma_i^{(+)} - \sigma_i^{(-)} \right)^2}, \quad \Delta\sigma_{\alpha_s} = \frac{1}{2} \sqrt{(\sigma(\alpha_s = 0.116) - \sigma(\alpha_s = 0.120))^2}$$

$$(\Delta\sigma)^2 = (\sigma_{\text{PDF}})^2 + (\sigma_{\alpha_s})^2$$

$gg \rightarrow H$ (pb), PDF unc.	8 TeV	13 TeV
68% C.L. (Hessian)	18.7 + 2.1% - 2.3%	42.7 + 2.0% - 2.4%
68% C.L. (LM)	+2.3% - 2.3%	+2.4% - 2.5%
$gg \rightarrow H$ (pb), PDF+ α_s	8 TeV	13 TeV
68% C.L. (Hessian)	18.7 + 2.9% - 3.0%	42.7 + 3.0% - 3.2%
68.0% C.L. (LM)	+3.0% - 2.9%	+3.2% - 3.1%

Table 1: Uncertainties of $\sigma_H(gg \rightarrow H)$ computed by the LM method and by the Hessian method, with Tier-2 penalty included. The 68% C.L. errors are given as percentage of the central value, and the PDF-only uncertainties are for $\alpha_s = 0.118$.

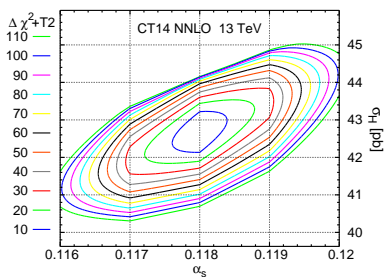
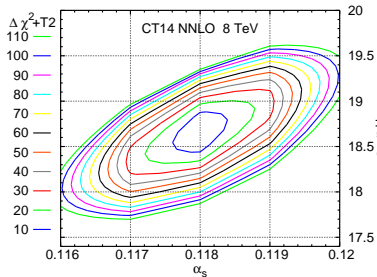
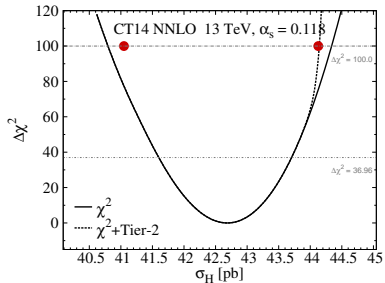
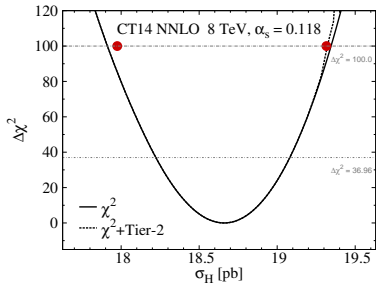
PDF uncertainties in $gg \rightarrow H$

- Most analyses use Hessian Method (n error PDF sets)

$$(\delta X)^2 = \frac{1}{4} \sum_{k=1}^n (X(a_k^+) - X(a_k^-))^2$$

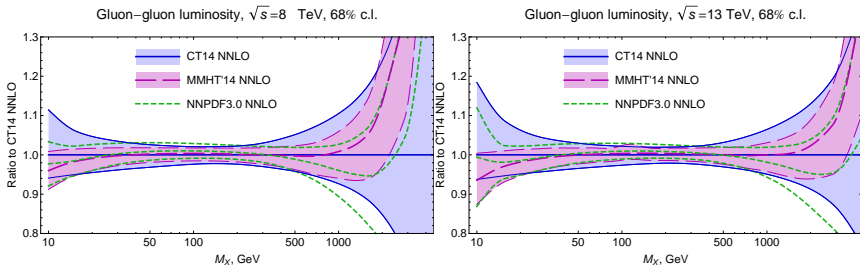
- Error sets can be used by anyone for any observable
 - Assume quadratic and linear dependence of χ^2 , X on a_k
- Lagrange Multiplier (LM) method is more robust
 - Find best fit for each constrained value of observable X
 - No assumptions on dependence of χ^2 , X on a_k
 - Can validate Hessian method
 - Can display correlations between PDFs and Observable
 - Must calculate separately for each observable

Lagrange Multiplier method in $gg \rightarrow H$



PDF uncertainties in $gg \rightarrow H$

8 TeV 13 TeV

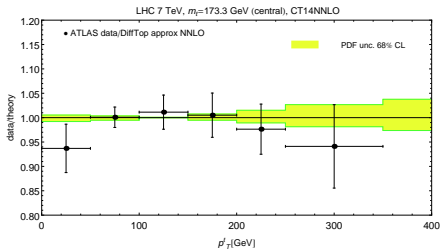
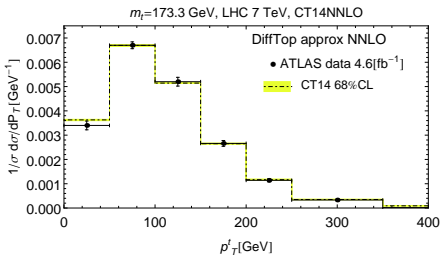


	CT14	MMHT2014	NNPDF3.0	CT10
8 TeV	$18.66^{+2.1\%}_{-2.3\%}$	$18.65^{+1.4\%}_{-1.9\%}$	$18.77^{+1.8\%}_{-1.8\%}$	$18.37^{+1.7\%}_{-2.1\%}$
13 TeV	$42.68^{+2.0\%}_{-2.4\%}$	$42.70^{+1.3\%}_{-1.8\%}$	$42.97^{+1.9\%}_{-1.9\%}$	$42.20^{+1.9\%}_{-2.5\%}$

Table 2: The Higgs boson production cross sections (in pb) for the gluon fusion channel at the LHC, at 8 and 13 TeV center-of-mass energies, using the CT14, MMHT2014, NNPDF3.0, and CT10 PDFs, with a common value of $\alpha_s(m_Z)$ of 0.118. The errors given are the PDF errors at the 68% confidence level.

$t\bar{t}$ cross section

ATLAS



CMS

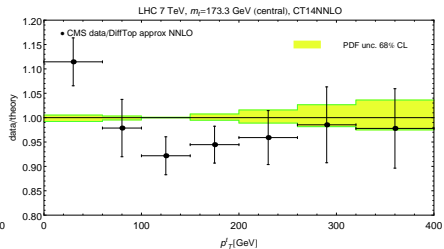
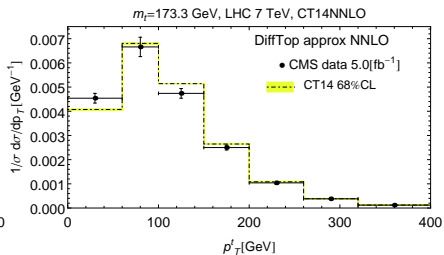


Figure 2: Final-state top-quark p_T differential distribution at ATLAS and CMS 7 TeV.

$t\bar{t}$ cross section

$pp \rightarrow t\bar{t}$ (pb), PDF unc.	8 TeV	13 TeV
68% C.L. (top++2.0)	250 + 3.9% - 3.5%	820 + 2.6% - 2.7%
68% C.L. (LM)	+4.8% - 4.6%	+2.9% - 2.9%
$pp \rightarrow t\bar{t}$ (pb), PDF+ α_s	8 TeV	13 TeV
68% C.L. (Hessian)	+5.2% - 4.4%	+3.6% - 3.5%
68% C.L. (LM)	+5.1% - 4.7%	+3.6% - 3.5%

Table 3: The $t\bar{t}$ total inclusive cross sections given in pb are evaluated at LHC center of mass energies of 8 and 13 and TeV with the TOP++2.0 code.

Not included in the global fit (and available only at NLO)

$t\bar{t}$ cross section

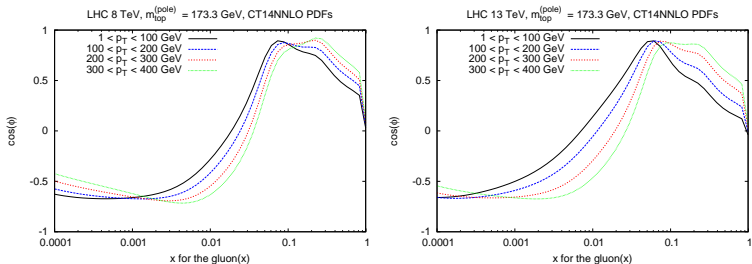


Figure 3: Theoretical correlation cosine as a function of x -gluon for the top-quark p_T distribution in $t\bar{t}$ production at the LHC at $\sqrt{s} = 8$ and 13 TeV.

$$\cos \varphi = \frac{\vec{\nabla} X \cdot \vec{\nabla} Y}{\Delta X \Delta Y} = \frac{1}{4 \Delta X \Delta Y} \sum_{i=1}^N \left(X_i^{(+)} - X_i^{(-)} \right) \left(Y_i^{(+)} - Y_i^{(-)} \right).$$

CMS $W+c$

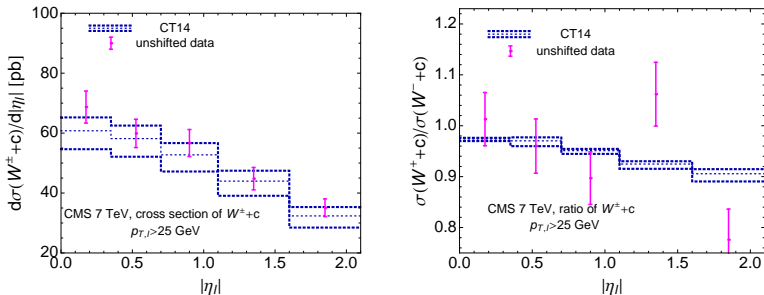
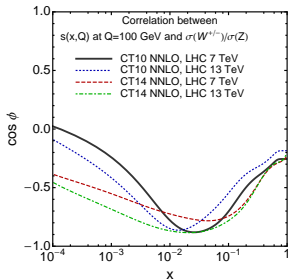
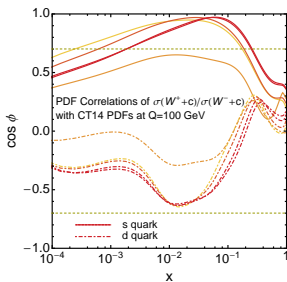
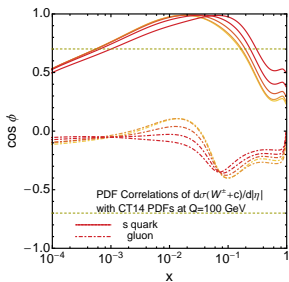


Figure 4: Comparison of the CT14 prediction for $W^\pm + c$ differential cross sections (left) and for the ratio of $W^+ + \bar{c}$ to $W^- + c$ cross sections (right) from the CMS measurement at 7 TeV.

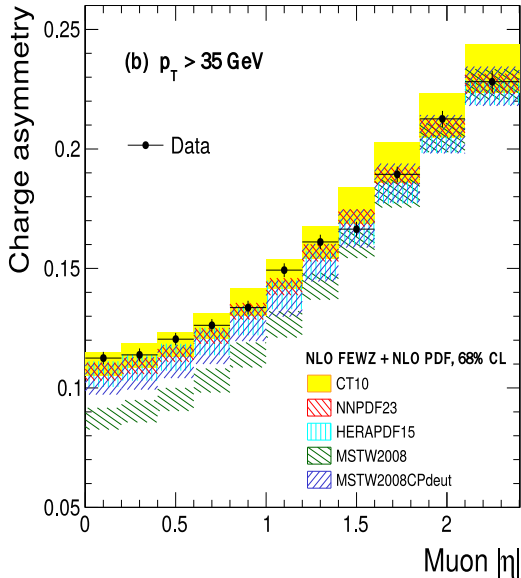
Not included in the global fit (and available only at NLO)

CMS $W+c$



The $W^\pm + c$ cross sections is more correlated to strange quark for $x = 0.01 - 0.1$.

CMS, $L = 4.7 \text{ fb}^{-1}$ at $\sqrt{s} = 7 \text{ TeV}$



Data is already more precise than current PDF uncertainty.

Will help to determine PDFs in small x region.

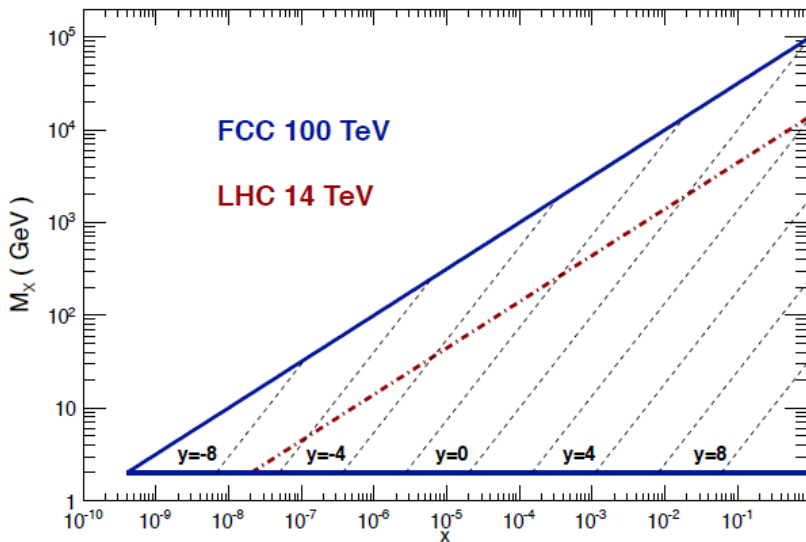
Most useful for determining \bar{d}/\bar{u} .

PDFs for Future Hadron Colliders

- Parton distribution function $f(x, Q)$
- Given a heavy resonance with mass Q produced at hadron collider with c.m. energy \sqrt{s}
- What's the typical x value? $\langle x \rangle = \frac{Q}{\sqrt{s}}$ at central rapidity ($y = 0$)
- Generally, $x_1 = \frac{Q}{\sqrt{s}} e^y$, $x_2 = \frac{Q}{\sqrt{s}} e^{-y}$,
 $x_1 + x_2 = 2 \frac{Q}{\sqrt{s}} \cosh(y)$, therefore $x_1 + x_2 = 1$

Kinematics of a 100 TeV FCC

Plot by J. Rojo, Dec 2013



J. Rojo: kickoff meeting for FCC at CERN, Feb. 2014

On to a 100 TeV SppC

will access smaller x , larger Q^2

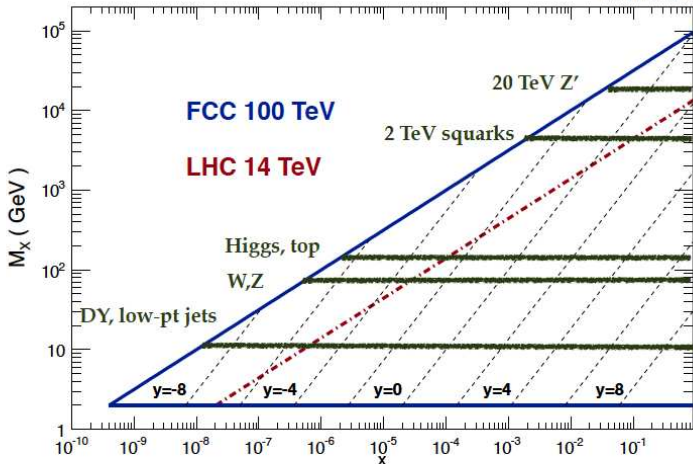
currently have no constraints on PDFs for x values below $1E-4$

poor constraints (still) as well for high x PDFs

at high masses (Q^2), rely on DLAP evolution; we know at large Q^2 , EW effects also become important

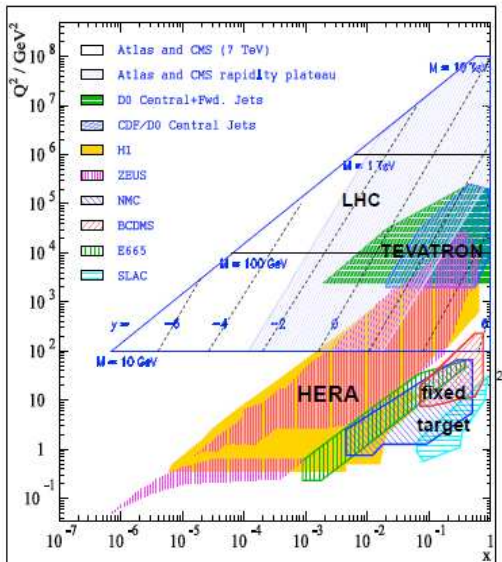
Kinematics of a 100 TeV FCC

Plot by J. Rojo, Dec 2013

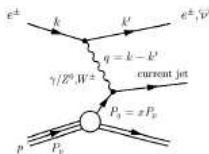


On to a 100 TeV SppC

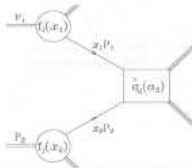
Experimental access to the proton structure



HERA: low and medium x



LHC: important constraints on $g(x)$, flavour separation

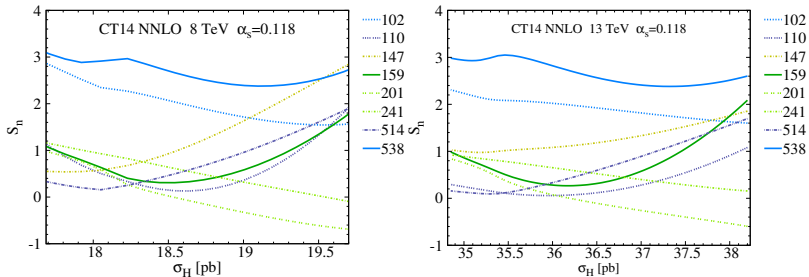


Fixed Target: high x , nuclear PDFs

Summary

- PDFs have larger uncertainties in both small x and large x regions.
- The eigen sets is useful for calculating the PDF induced uncertainty, and correlation between observables.
- PDFs will be further determined by LHC data.

Backup



The S_n is the effective Gaussian variable which present the goodness of fit of particular data.